JOURNAL OF APPLIED ELECTROCHEMISTRY 24 (1994) 332–336

Kinetics of lead deposition in fluorosilicate electrolyte Part II: Inhibiting effect of horse-chestnut extract (HCE) and of sodium lignin sulphonate–HCE mixtures

L. MURESAN, L. ONICIU

University of Cluj-Napoca, Faculty of Chemistry, 3400 Cluj-Napoca, Romania

R. WIART

UPR15 du CNRS, Physique des Liquides et Electrochimie, Université Pierre et Marie Curie, Tour 22, 4 place Jussieu, 75252 Paris, Cedex 05, France

Received 29 March 1993; revised 23 August 1993

The kinetics of lead electrodeposition from Betts-type electrolytes were investigated by electrochemical impedance spectroscopy, in the presence of some organic levelling agents: horse chestnut extract (HCE) and mixtures of HCE with sodium lignin sulphonate (LS). The impedance spectra and the polarization curves are influenced by the electrode rotation speed and the electrolyte composition. In Part I, a reaction model for lead electrodeposition was shown to be valid in additive-free fluorosilicate electrolytes or in the presence of LS alone. To account for the specific inhibition observed with HCE, this model is completed by addition of a diffusion-controlled process for adsorption and consumption of the HCE molecules at the cathode during lead deposition.

1. Introduction

To obtain smooth lead deposits, lead electrorefining from fluorosilicate electrolytes takes place in the presence of various organic compounds which act as levelling agents. It has been shown that sodium lignin sulphonate (LS) and an extract of horse chestnut (HCE) have a beneficial effect on the quality of lead deposits [1, 2].

In previous work, the inhibiting influence of the LS additive was studied by using electrochemical impedance spectroscopy and polarization curves and it was interpreted in terms of changes in the kinetic parameters of the reactions leading to lead deposition [3]. The proposed reaction path implied a direct discharge of $PbSiF_6$ species coupled to the formation of the complex species $[SiF_6(X)]^{2-}$ existing only in the proximity of the electrode; here X denotes a proton or a LS molecule. These complex species can be adsorbed on the electrode surface, thus covering a fraction, θ, of the area. The complex species may inhibit the charge transfer reaction or it can diffuse towards the bulk electrolyte. The diffusion process being slow in comparison with the adsorption–desorption equilibrium, a rise in the coverage, θ, with increasing potential generates a faradaic capacitive impedance characterized by the diffusion time constant.

The adsorption of LS molecules decreases both the double layer capacity and the activation coefficient of the charge transfer reaction with potential. It also stabilizes the number of active sites for lead deposition, whose potential activation is connected with the inductive feature observed in the additive-free electrolyte.

The aim of the present work is to investigate the kinetics of lead electrocrystallization in fluorosilicate electrolyte in the presence of horse chestnut extract used alone or in combination with lignin sulphonate, by means of impedance measurements. The reaction path is described to account for the experimental features observed in the presence of these levelling agents and to interpret the synergetic effect of LS and HCE mixtures.

2. Experimental procedure

The electrolytes were analytical grade reagents dissolved in double ion-exchanged water and the concentrations were 80 g dm^{-3} H_2SiF_6 and 80 g dm^{-3} Pb^{2+} as $PbSiF_6$. The alcoholic extract of horse chestnut seeds was prepared in the laboratory according to a patented method [4]. When used alone, the concentration of HCE was 3 g dm^{-3}. In the various LS + HCE mixtures, the concentration of LS was of 3 g dm^{-3} and the HCE concentration was varied between 1 and 6 g dm^{-3}.

The electrochemical cell was provided with a rotating titanium disc electrode of surface area 1.13 cm^2, a large pure lead sheet as counter electrode and a saturated calomel reference electrode (SCE) with a KNO_3 salt bridge. The electrode rotation speed was electronically controlled and varied from 100 to 1200 r.p.m. The cell temperature was held at

0021-891X 1994 Chapman & Hall

25 ± 0.5° C. The use of a titanium substrate is known to allow an easy detachment of the lead deposit. In the present work, the deposit thickness was sufficient to investigate the kinetics of lead deposition on lead, independently of the substrate.

The electrode impedance was measured under potentiostatic conditions using a frequency response analyser Solartron 1174, between 12 mHz and 60 kHz. The steady-state current/potential curves were plotted from the current and potential values measured during the impedance measurements and were corrected for ohmic drop.

3. Results

3.1. *Current–potential curves*

As shown in Fig. 1, in the presence of HCE and of different HCE + LS mixtures, the general form of the polarization curves is modified in comparison with their form in the absence of additives or in the presence of LS alone. It appears that the HCE, used in the same concentration as LS in the previous experiments (3 g dm^{-3}) [3], induces a larger cathodic overpotential and drastically reduces the reaction rate. In the presence of HCE + LS mixtures, the shift of the polarization curves towards negative potentials is less than in the case of HCE alone: the curves are located between those corresponding to LS alone and HCE alone, respectively.

It must be emphasized that both in the presence of HCE alone or in mixtures with LS, at less negative potentials ($E > -0.6$ V vs SCE) the current decreases with increasing rotation speed, thus indicating that the inhibition process is controlled by the diffusion of HCE towards the cathode (Fig. 2). In this potential range, a linear dependence of I upon $\Omega^{1/2}$ is

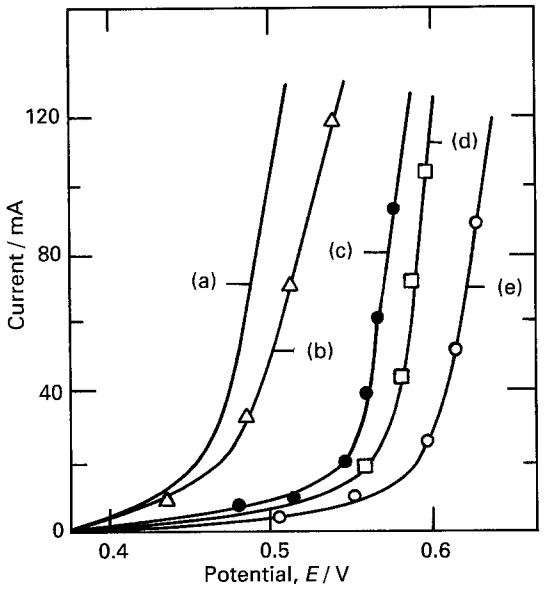

Fig. 1. Polarization curves corrected for ohmic drop. Rotation speed 1200 r.p.m. (a) Additive-free electrolyte; (b) with 3 g dm^{-3} LS; (c) with 3 g dm^{-3} LS + 3 g dm^{-3} HCE; (d) with 3 g dm^{-3} LS + 6 g dm^{-3} HCE; (e) with 3 g dm^{-3} HCE.

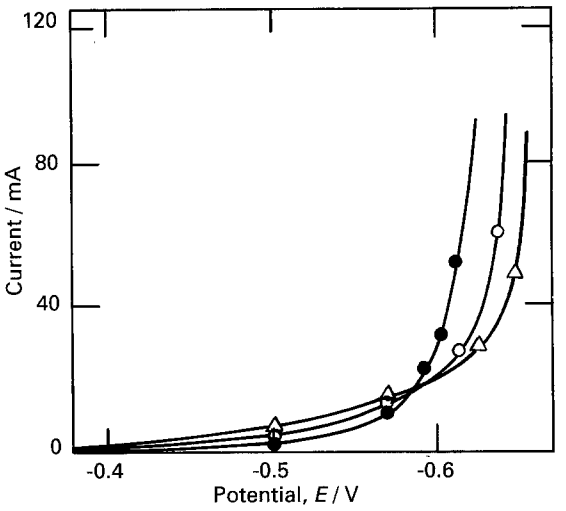

Fig. 2. Polarization curves corrected for ohmic drop in the presence of 3 g dm^{-3} HCE, at various rotation speeds: (△) 100 r.p.m.; (○) 400 r.p.m. and (●) 1200 r.p.m.

observed, as predicted by the rotating disc electrode theory [5] (Fig. 3).

At more negative potentials ($E < -0.6$ V vs SCE), the current increases with rotation speed, as in the cases without additive and with LS [3]. This effect of the rotation speed on the current becomes more pronounced with increasing HCE concentration.

At the cross-over of curves ($E \approx -0.6$ V vs SCE), the diffusion of HCE towards the electrode is balanced by the influence of the complex fluorosilicate species which diffuse away [3] and the electrodeposition process is independent of the hydrodynamic conditions.

3.2. *Impedance diagrams*

The impedance diagrams recorded over the whole polarization range, exhibit two capacitive features which predominate at low cathodic potentials (Fig. 4(a)), and an additional low-frequency inductive loop at the higher negative potentials corresponding

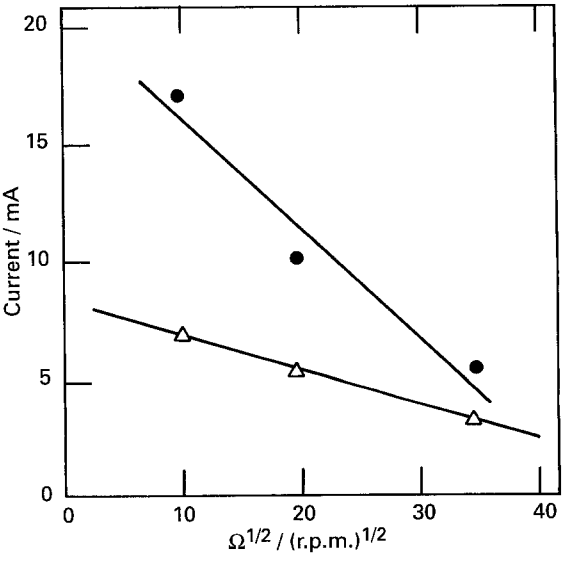

Fig. 3. Current variation with the square root of the rotation speed of the electrode in the presence of 3 g dm^{-3} HCE at low cathodic overpotentials. (●) $E = -0.543$ V; (△) $E = -0.496$ V.

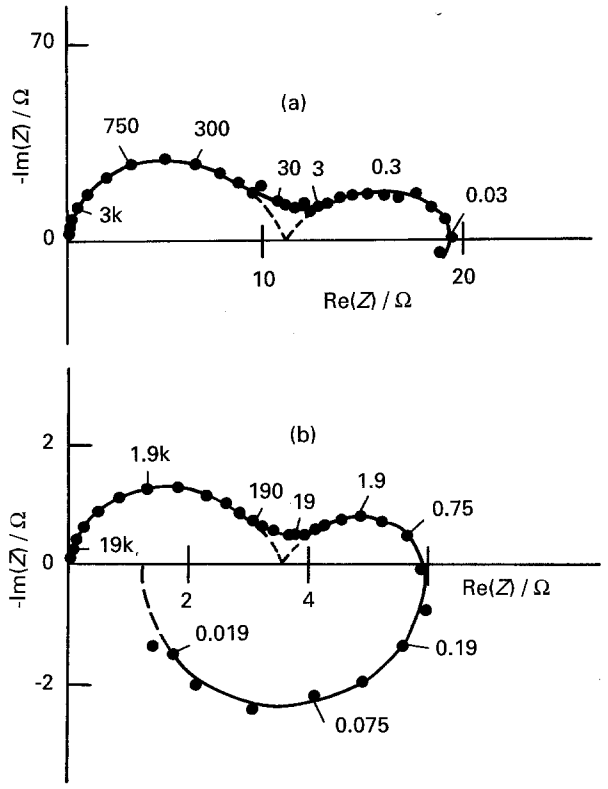

Fig. 4. Complex plane impedance plots recorded in the presence of 3 g dm^{-3} HCE. Rotation speed 1200 r.p.m. (a) Potential $E = -0.54$ V, $I = 5.6$ mA, (b) Potential $E = -0.60$ V, $I = 21.5$ mA.

to the steep slope of the polarization curves (Fig. 4(b)). The mean double layer capacity calculated from the apex of the high frequency capacitive loop is situated between 30 and 50 μF cm^{-2} in the presence of HCE alone and between 20 and 50 μF cm^{-2} in the presence of different mixtures LS + HCE. These values are close to that measured in the presence of LS alone, 40 μF cm^{-2}. The electrolyte resistance, R_e, was about 1.1 Ω in the presence of 3 g dm^{-3} HCE and between 1.1 and 1.9 Ω in the presence of different mixtures of LS + HCE. The R_tI product of the charge

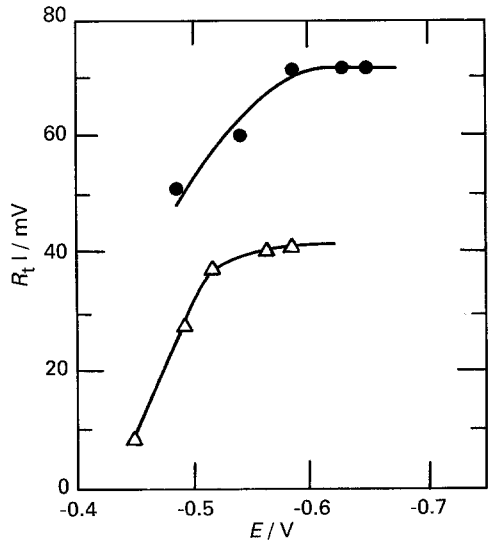

Fig. 5. Potential dependence of the R_tI product for the electrolyte with 3 g dm^{-3} HCE (●) and with 3 g dm^{-3} HCE + 3 g dm^{-3} LS (△). Rotation speed 1200 r.p.m.

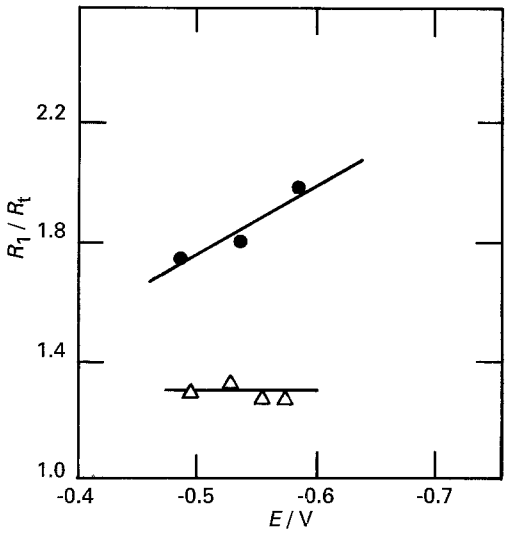

Fig. 6. Potential dependence of the R_1/R_t ratio: (●) electrolyte with 3 g dm^{-3} HCE; (△) electrolyte with 3 g dm^{-3} LS + 3 g dm^{-3} HCE. Rotation speed 1200 r.p.m.

transfer resistance, R_t, and the current, I, first increases with electrode polarization and then tends towards an approximately constant value around 70 mV in the presence of HCE alone and around 40 mV in the presence of various mixtures LS + HCE (Fig. 5).

According to the relatively high value of the charge transfer resistance, R_t, the frequency at the apex of the high-frequency capacitive loop, f_0, is much smaller than in the absence of additive or in the presence of LS. The frequency f_0 increases with the potential, whereas the frequency, f_1, characteristic of the low-frequency capacitive loop is nearly constant.

As in the case without additive and in the presence of LS alone [3], the size of the low-frequency capacitive loop, described by the R_1/R_t ratio, where R_1 is the resistance corresponding to the intermediate frequency at the end of the low-frequency capacitive loop, increases with the electrode polarization (Fig. 6) in the presence of HCE alone. In contrast, it remains potential independent when LS and HCE

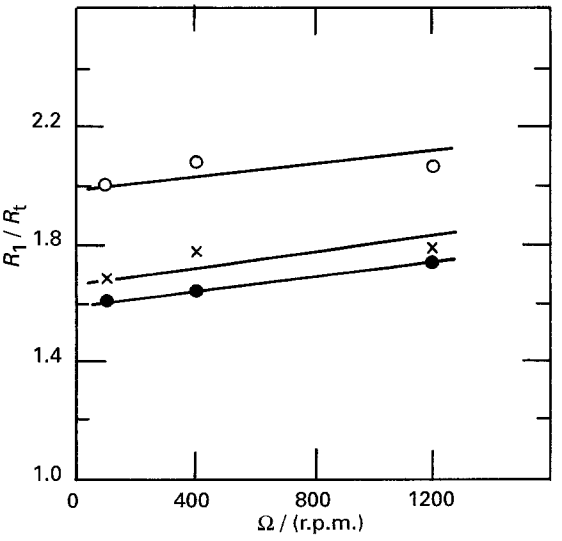

Fig. 7. Rotation speed dependence of the R_1/R_t ratio for an electrolyte with 3 g dm^{-3} HCE; (●) $E = -0.500$ V; (×) $E = -0.550$ V; (○) $E = -0.600$ V.

are used together. On the other hand, the R_l/R_t ratio slightly increases with the electrode rotation speed Ω (Fig. 7).

4. Discussion

4.1. *Influence of HCE*

The mechanism to account for the results obtained in the presence of HCE has to take into account the particular behaviour of the system observed in the range of low polarizations ($E > -0.6$ V vs SCE) where the inhibition of the electrodeposition process increases with rotation speed.

In the presence of HCE, the reaction path I

$$PbSiF_6 + X + 2e^- \xrightarrow{K_1} Pb + [SiF_6X]^{2-} \quad (I)$$

$$\xrightarrow{D} (SiF_6^{2-} + X)_{sol} K \downarrow\uparrow K'[SiF_6X]^{2-}_{ads}$$

taking place in additive-free electrolyte or in LS-containing electrolyte [3] must be combined with the slow process (II) for the inhibition by HCE

$$HCE_{sol} \xrightarrow{D'} HCE \xrightarrow{K_a} HCE_{ads} \xrightarrow{K_c} HCE_{consumed} \quad (II)$$

In path I, X possibly denotes H^+ or the complexing LS molecules, and the adsorbate $[SiF_6X]^{2-}_{ads}$ covers a fraction, θ, of the electrode surface. Path II involves three steps: (i) the diffusion of HCE towards the electrode, (ii) the adsorption step K_a which forms the inhibiting adsorbate HCE_{ads} and (iii) the consumption step K_c of HCE_{ads} by decomposition or inclusion coupled to the deposition process of lead.

A diffusion-controlled inhibition of electrodeposition by an additive is known to be the preponderant mechanism for levelling [6], and both the inhibition by adsorbed molecules and their consumption rate are then simultaneously controlled by diffusion [7, 8]. If the consumption of HCE molecules is diffusion controlled ($K_a \gg D'/\delta$), the mass balance of HCE molecules, of concentration c_0 and c near the cathode and in the bulk of electrolyte, respectively, can be written as

$$\frac{D'c}{\delta} = K_a c_0(1 - \theta - \theta_1) = K_c\theta_1 \quad (1)$$

where D' is the diffusion coefficient of HCE molecules, δ is the thickness of the diffusion layer and θ_1 is the electrode coverage by HCE_{ads}. For the rotating disc electrode,

$$\theta_1 = \frac{D'c}{\delta K_c} = \frac{0.62D'^{2/3}c\nu^{-1/6}}{K_c}\Omega^{1/2} \quad (2)$$

The current density, i, corresponding to the reaction path I is [3]

$$i = 2FK_1C(1 - \theta - \theta_1) \quad (3)$$

where C is the concentration of $PbSiF_6$ and $K_1 = k_1 \exp(b_1E)$ denotes the rate constant of lead deposition which follows a Tafel activation with cathodic potential E.

At low current densities, the coverage θ by $[SiF_6X]^{2-}_{ads}$ is low [3], and it may be assumed that the inhibition mainly results from θ_1. Therefore, i takes the form

$$i = 2FK_1C(1 - a\Omega^{1/2}) \quad (4)$$

where a is a constant. Equation 4 implies a linear decrease of i with increase in $\Omega^{1/2}$, the slope being an increasing function of the electrode potential, in agreement with the experimental data in Fig. 3.

From Equation 3, two distinct relaxation processes in the faradaic impedance Z_F can be predicted:

$$\frac{1}{Z_F} = \frac{1}{R_t} + \left(\frac{\partial i}{\partial\theta}\right)_{\theta_1,E}\frac{\Delta\theta}{\Delta E} + \left(\frac{\partial i}{\partial\theta_1}\right)_{\theta,E}\frac{\Delta\theta_1}{\Delta E} \quad (5)$$

The charge transfer resistance, R_t, is such that

$$R_t i = 1/b_1 \quad (6)$$

The values of $R_t i$ product corresponding to the plateaux in Fig. 5 give the activation parameter b_1 of K_1. For an electrolyte containing 3 g dm^{-3} HCE, the value of $b_1 = 14\,V^{-1}$ is much lower than for the additive-free electrolyte, thus indicating a strong inhibiting influence of HCE at the stage of the charge transfer reaction.

In Equation 5, the term $[-i/(1 - \theta - \theta_1)]\Delta\theta/\Delta E$ generates a capacitive feature, since θ has been shown to be an increasing function of E [3], and the resistance R_1, which defines the size of this capacitive loop, is given by

$$\frac{R_1}{R_t} = 1 + \frac{i}{(1 - \theta - \theta_1)}\frac{d\theta}{di} \quad (7)$$

where $d\theta/di$ denotes the steady-state variation of θ.

The shape of the low-frequency capacitive loop in Fig. 4 agrees with a partial diffusion control of the coverage θ, as already shown for the additive-free electrolyte [3], although no significant dependency of the characteristic frequency upon the electrode rotation speed has been detected in the presence of HCE. As shown in Fig. 4, this frequency (0.3 Hz and 1.9 Hz on impedance plots in Fig. 4) has the same magnitude as for the additive-free electrolyte. In addition, in view of the predominance of the coverage θ_1, which is proportional to $\Omega^{1/2}$, in the inhibition process, Equation 7 accounts for an increase in the ratio R_1/R_t with increasing Ω.

At relatively high current densities, it can be reasonably assumed that the consumption of HCE_{ads} occurs by inclusion into the lead deposit and then the consumption rate becomes proportional to the current density, i.e. $K_c i\theta_1$, as already proposed in the literature [7, 8]. Changing K_c into $K_c i$ in Equations 1 and 2 yields a new definition of θ_1:

$$\theta_1 = \frac{D'c}{\delta K_c i} \quad (8)$$

and it is clear that a decrease of θ_1 with increasing i generates an inductive feature, due to the desorption of HCE_{ads}. Such a desorption process, activated

with increasing current, results in an increase in the number of active sites for lead deposition, which was formally invoked in the case of the additive-free electrolyte [3].

The inhibition process (II) allows the mass balance of adsorbed HCE molecules to be expressed as

$$\beta \frac{d\theta_1}{dt} = K_a c_0 (1 - \theta - \theta_1) - K_c i \theta_1 \quad (9)$$

where β is the maximum surface concentration of adsorbed species, and under steady-state conditions

$$\theta_1 = \frac{K_a c_0 (1 - \theta)}{K_a + K_c i} \quad (10)$$

Considering that the relaxation of θ_1 is much slower than that of θ, the polarization resistance R_p, corresponding to Z_F for $\omega = 0$, is given by

$$\frac{1}{R_p} = \frac{1}{R_1} - \frac{i}{(1 - \theta - \theta_1)} \frac{d\theta_1}{R_p \, di} \quad (11)$$

or

$$\frac{R_p}{R_1} = 1 + \frac{i}{(1 - \theta - \theta_1)} \frac{d\theta_1}{di} \quad (12)$$

Since θ_1 is a decreasing function of i, $R_p < R_1$, which is consistent with an inductive feature due to the relaxation of θ_1. The time constant, τ, characteristic of this inductive feature is given by a linearization of Equation 9:

$$(K_a c_0 + K_c i)(1 + j\omega\tau)\Delta\theta_1 = K_a (1 - \theta - \theta_1)\Delta c_0 - K_a c_0 \Delta\theta - K_c \theta_1 \Delta i \quad (13)$$

where

$$\tau = \frac{\beta}{K_a c_0 + K_c i} \quad (14)$$

is defined from the low rate constants of the adsorption–consumption process.

At high polarizations, the inhibition of lead deposition by HCE_{ads} vanishes since θ_1 decreases. Thus the inhibiting effect of $[SiF_6X]^{2-}_{ads}$ becomes progressively more efficient and generates an increase in i with increasing Ω, observed on the polarization curves (Fig. 2) and similar to the situation reported in the additive-free electrolyte or in the presence of LS [3].

4.2. *Influence of LS and HCE mixtures*

Considering the results obtained in electrolytes containing mixtures of LS (at a concentration of $3\,g\,dm^{-3}$) and HCE at various concentrations, an intermediate situation was observed between the two cases of LS alone or HCE alone. The relative position of the polarization curves in the presence of each of the two additives used separately, as compared with the curves obtained in the presence of LS + HCE mixtures, suggests the existence of a competitive adsorption of the two organic compounds at the interface. Thus a certain ratio between the concentrations of the two additives must be realized at the interface.

This idea is also supported by the fact that the two compounds do not act in the same manner on the electrodeposition process: LS moderately inhibits the charge transfer reaction ($b_1 = 25\,V^{-1}$) and blocks the number of active sites on the metal surface, while HCE strongly inhibits the charge transfer reaction ($b_1 = 14\,V^{-1}$) and allows a moderate and controlled increase in the number of active sites due to a vanishing inhibition with increasing current. It is likely that an optimal levelling of lead deposits is attained in the presence of an optimized concentration of each of the levelling agents. This concentration should ensure a moderate activation overpotential and a moderate variation of the number of active sites with the potential.

Hydrodynamic conditions in the electrorefining cell are also important, since the coverage with LS decreases with increasing stirring rate, while the coverage with HCE increases with stirring rate, mainly in the range of low cathodic overpotentials. Thus, it is probable that the optimum of the LS/HCE concentrations ratio can be realized by appropriate stirring of the electrolyte.

Thus it is possible to define experimental conditions leading to a good balance between the specific action of the two additives. The optimum concentration ratio in the electrorefining cell is observed to be $3\,g\,dm^{-3}$ LS to $2–3\,g\,dm^{-3}$ HCE. In conclusion, it seems that the synergism observed with the use of both LS and HCE in the same electrolyte results from their specific action in the different stages of the electrocrystallization process and from their opposite dependence on electrolyte stirring.

References

[1] L. Ghergari, L. Oniciu, L. Muresan, A. Pantea, V. A. Topan and D. Ghertoiu, *J. Electroanal. Chem.* **313** (1991) 303–311.

[2] L. Muresan, L. Oniciu, M. Froment and G. Maurin, *Electrochim. Acta* **37** (1992) 2249–2254.

[3] L. Muresan, R. Wiart and L. Oniciu, *J. Appl. Electrochem.* **23** (1993) 66.

[4] L. Oniciu, L. Muresan, V. A. Topan and D. Ghertoiu, *Rom. Pat.* **104** (1991) 946.

[5] V. G. Levitch, 'Physicochemical Hydrodynamics', Prentice Hall, New York (1962).

[6] O. Kardos, *Plating* **61** (1974) 129, 229 and 316.

[7] J. Edwards, *Trans. Inst. Metal Finish* **41** (1964) 140.

[8] S. S. Kruglikov, Yu. D. Gamburg and N. T. Kudryavtsev, *Electrochim. Acta* **12** (1967) 1129.